

Structure of New Layered Oxides $M^{II}_{0.5}LaTiO_4$ ($M = Co, Cu, \text{ and } Zn$) Synthesized by the Ion-Exchange Reaction

Sun Young Kim,[†] Jong-Min Oh,[†] Jung-Chul Park,[‡] and Song-Ho Byeon^{*,†}

College of Environment and Applied Chemistry, Institute of Natural Sciences, Kyung Hee University, Kyung Ki 449-701, Korea, and Department of Chemistry of New Materials, Silla University, Pusan 617-736, Korea

Received October 1, 2001. Revised Manuscript Received January 3, 2002

New layered oxides $M^{II}_{0.5}LaTiO_4$ ($M = Co, Cu, \text{ and } Zn$) were synthesized via the ion-exchange reaction of parent $NaLaTiO_4$ in molten salts at 300–450 °C. Eutectic-like mixtures of MCl_2 ($M = Co \text{ and } Cu$) and KCl were required for the 1:2 exchange reaction of divalent cobalt and copper ions for monovalent sodium ion at low temperature. The structures of these phases were determined by Rietveld refinement of the powder X-ray and neutron diffraction data. The bright violet ($M = Co$), bright brown ($M = Cu$), and white ($M = Zn$) compounds crystallize in the tetragonal structure (space group $P4/nmm$) with cell constants $a = 3.71379(6), 3.73606(9), \text{ and } 3.7234(1) \text{ \AA}$ and $c = 12.7016(2), 12.0736(3), \text{ and } 12.7488(6) \text{ \AA}$, respectively. Similarly to the structure of parent $NaLaTiO_4$, a strongly distorted coordination environment for the Ti atom is revealed. In contrast, the transition metal atoms statistically occupy one-half of the distorted tetrahedral sites rather than the nine-coordinated sites in the interlayer spaces. Successful syntheses of $M^{II}_{0.5}LaTiO_4$ and $M^{II}La_2Ti_3O_{10}$ suggest the existence of various colored layer-type oxide family of general formula $M^{II}[A_{n-1}B_nO_{3n+1}]$ ($M = \text{transition metals}$).

Introduction

Several families^{1–5} of perovskite-related oxides with layered structures have been of great interest for their diverse crystallographic, chemical, and physical properties.^{6–15} They are dubbed the Aurivillius phases, Ruddlesden–Popper (RP) phases, and Dion–Jacobson (DJ) phases. These series are generally described as multiple perovskite slabs interleaved by cation layers with a different structure. Even though numerous

layered perovskite oxides are known at present, novel members with new structural types and new properties are being continually added to the growing list of perovskite derivatives.^{16–22}

As part of a program designed to develop new layered perovskite families using a low-temperature topotactic route, we recently reported the synthesis of $M^{II}La_2Ti_3O_{10}$ ($M = Co, Cu, \text{ and } Zn$) by the ion-exchange reaction of parent $Na_2La_2Ti_3O_{10}$ in a eutectic-like molten salt.²³ Considering that the structural type of layered perovskites is generally determined by large ions, the structure of $M^{II}La_2Ti_3O_{10}$ is quite unusual because it retains a typical RP structure even after the large cations are replaced by much smaller ones. If the sodium layers in $Na_2La_2Ti_3O_{10}$ were exchanged by transition metal ions, the same methodology could be extended to different RP members with alkali metal layers. Such a generalized exchange reaction would then be expected to result in the formation of a new perovskite-related family. Accordingly, in this work, we explored the synthesis of a series of layered perovskites, $M^{II}_{0.5}LaTiO_4$ ($M = \text{transition metals}$). The parent oxide $NaLaTiO_4$

* To whom all correspondence should be addressed.

[†] Kyung Hee University

[‡] Silla University

- (1) Aurivillius, B. *Ark. Kemi.* **1949**, *1*, 463; **1950**, *2*, 519.
- (2) Ruddlesden, S. N.; Popper, P. *Acta Crystallogr.* **1957**, *10*, 538; **1958**, *11*, 54.
- (3) Jacobson, A. J.; Johnson, J. W.; Lewandowski, J. T. *Inorg. Chem.* **1985**, *24*, 3727.
- (4) Dion, M.; Ganne, M.; Tournoux, M. *Mater. Res. Bull.* **1981**, *16*, 1429.
- (5) Dion, M.; Ganne, M.; Tournoux, M. *Rev. Chim. Miner.* **1986**, *23*, 61.
- (6) Gopalakrishnan, J.; Bhat, V.; Raveau, B. *Mater. Res. Bull.* **1987**, *22*, 413.
- (7) Subramanian, M. A.; Gopalakrishnan, J.; Sleight, A. W. *Mater. Res. Bull.* **1988**, *23*, 837.
- (8) Domen, K.; Yoshimura, J.; Sekine, T.; Tanaka, A.; Onishi, T. *Catal. Lett.* **1990**, *4*, 339.
- (9) Uma, S.; Raju, A. R.; Gopalakrishnan, J. *J. Mater. Chem.* **1993**, *3*, 709.
- (10) Armstrong, A. R.; Anderson, P. A. *Inorg. Chem.* **1994**, *33*, 4366.
- (11) Moritomo, Y.; Asamitsu, A.; Kuwahara, H.; Tokura, Y. *Nature* **1996**, *380*, 141.
- (12) Byeon, S.-H.; Yoon, J.-J.; Lee, S.-O. *J. Solid State Chem.* **1996**, *127*, 119.
- (13) Seshadri, R.; Martin, C.; Hervieu, M.; Raveau, B.; Rao, C. N. R. *Chem. Mater.* **1997**, *9*, 270.
- (14) Takano, Y.; Takayanagi, S.; Ogawa, S.; Yamadaya, T.; Mori, N. *Solid State Commun.* **1997**, *103*, 215.
- (15) Ikeda, S.; Hara, M.; Kondo, J. N.; Domen, K.; Takahashi, H.; Okubo, T.; Kakihana, M. *Chem. Mater.* **1998**, *10*, 72.

- (16) Uma, S.; Gopalakrishnan, J. *Chem. Mater.* **1994**, *6*, 907.
- (17) Bohnke, C.; Bohnke, O.; Fourquet, J. L. *J. Electrochem. Soc.* **1997**, *144*, 1151.
- (18) Toda, K.; Takahashi, M.; Teranishi, T.; Ye, Z.; Sato, M.; Hinatsu, Y. *J. Mater. Chem.* **1999**, *9*, 799.
- (19) Bhuvanesh, N. S.; Crosnier-Lopez, M. P.; Duroy, H.; Fourquet, J. L. *J. Mater. Chem.* **1999**, *9*, 3093.
- (20) Floros, N.; Michel, C.; Hervieu, M.; Raveau, B. *J. Mater. Chem.* **1999**, *9*, 3101.
- (21) Crosnier-Lopez, M. P.; Duroy, H.; Fourquet, J. L. *Mater. Res. Bull.* **1999**, *34*, 179.
- (22) Bhuvanesh, N. S.; Crosnier-Lopez, M. P.; Bohnke, O.; Emery, J.; Fourquet, J. L. *Chem. Mater.* **1999**, *11*, 634.
- (23) Hyeon, K.-A.; Byeon, S.-H. *Chem. Mater.* **2000**, *11*, 352.

used for this work shows a peculiar structure such that the LaO and ion-exchangeable NaO layers are alternately ordered perpendicular to the c axis.^{24,25} Thus, a considerable charge imbalance exists between the two layers. Although the partial exchange reaction between divalent calcium ions and monovalent sodium ions of similar size has already been attempted with this oxide,²⁶ no reports have addressed an exchange reaction with much smaller divalent transition metal ions. This reaction should be unfavorable because the significant rearrangement and vacancy formation induced by such a complete 1:2 exchange in the interlayer spaces will considerably decrease the structural stability of the host material with its strong charge imbalance. Fortunately, the exchange reaction between sodium ions and some divalent transition metal ions was successfully carried out at low temperature by using a eutectic-like salt that was obtained by mixing KCl and MCl_2 in the appropriate ratio. Herein, we describe in detail the synthesis and structure of new layered perovskite compounds $M^{II}_{0.5}LaTiO_4$ ($M = Co, Cu, \text{ and } Zn$). Successful exchange reactions between sodium and transition metal ions in the interlayer spaces of two members ($NaLaTiO_4$ and $Na_2La_2Ti_3O_{10}$) of the RP family suggest the formation of a new series of layered oxides with the general formula $M^{II}[A_{n-1}B_nO_{3n+1}]$ ($M = \text{transition metals}$).

Experimental Details

Synthesis. The parent layered perovskite, $NaLaTiO_4$, was prepared by conventional solid-state reaction.²⁴ A mixture of Na_2CO_3 , La_2O_3 , and TiO_2 was heated in air at 850 °C for 20 h with one intermittent grinding. An excess (~20 mol %) of Na_2CO_3 was added to compensate for the loss of the volatile sodium component. After the reaction, the remaining sodium component was removed by washing with distilled water, and the product was dried at 120 °C.

A eutectic-like mixture of MCl_2 and KCl was required for the 1:2 exchange reaction of cobalt and copper ions for sodium ion at low temperature because of the high melting temperatures of $CoCl_2$ (mp = 735 °C) and $CuCl_2$ (mp = 620 °C). For the preparation of $Co_{0.5}LaTiO_4$, 1 g of $NaLaTiO_4$ was treated with 30 g of a molten mixture with a molar composition of 50% $CoCl_2$ and 50% KCl at 420 °C for 1 week. Similarly, $Cu_{0.5}LaTiO_4$ was prepared by treating 1 g of $NaLaTiO_4$ with 30 g of a molten mixture with a molar composition of 60% $CuCl_2$ and 40% KCl at 360 °C for 5 days. In contrast, $Zn_{0.5}LaTiO_4$ was easily prepared without addition of KCl by heating 1 g of $NaLaTiO_4$ with 10 g of molten $ZnCl_2$ (mp = 283 °C) at 300 °C for 10 days. All of the mixtures were replaced once during the course of the reaction. To avoid the formation of the corresponding MO oxides on heating MCl_2 in air, the Pyrex flask containing the reactants was filled with Ar gas throughout the reaction. After the exchange reaction of cobalt and copper ions for sodium ion, the oxide turned from white to bright violet and bright brown, respectively. The excess chlorides were washed from the final products with hot water.

Characterization. The absence of the sodium component and the stoichiometric composition of the transition metals in the ion-exchanged products were confirmed by inductively coupled plasma (ICP). No potassium component was detected, and the possibility of an exchange reaction between sodium

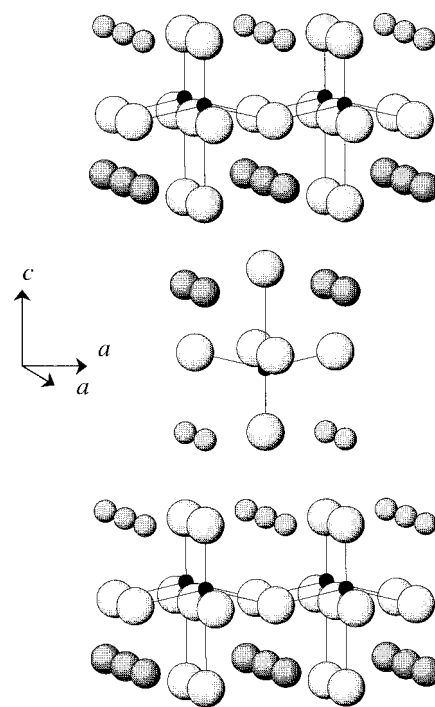


Figure 1. Illustration of the parent $NaLaTiO_4$ perpendicular to the c direction of the tetragonal unit cell. Only Ti–O bonds are shown by lines (Na = small shaded spheres, La = large shaded spheres, Ti = small black spheres, and O = large white spheres).

and potassium ions could accordingly be ruled out. Elemental analysis using the energy-dispersive X-ray emission (EDX) technique also gave a stoichiometric composition for the Co and Cu compounds (Co or Cu/La/Ti = 1:2:2) within experimental error.

Structure Analysis. The crystal structure was determined by powder X-ray and neutron diffraction. X-ray diffraction data for structure refinement were recorded on a rotating anode installed diffractometer with an X-ray source of 40 kV and 300 mA. The Cu $K\alpha$ radiation used was monochromatized by curved-crystal graphite. The intensity data were collected with a step-scan procedure in the range $2\theta = 10\text{--}110^\circ$ with a step width of 0.02° and a step time of 1 s. Neutron powder diffraction measurements were performed on the high-resolution powder diffractometer (HRPD) at the HANARO center of the Korea Atomic Energy Research Institute (KAERI). Refinement of the reflection positions and intensities was carried out using the Rietveld analysis program RIETAN.²⁷

Results and Discussion

Synthesis. The well-known Ruddlesden–Popper family is described by the general formula $A'_2[A_{n-1}B_nO_{3n+1}]$.^{2,28} One member ($n = 3$) of this family, $Na_2[La_2Ti_3O_{10}]$, has been used as a parent material for the synthesis of $M^{II}[La_2Ti_3O_{10}]$ via the ion-exchange reaction.²³ The stacking sequence of perovskite layers in these oxides retains the characteristics of the RP type, but their interlayer positions are half-occupied by small divalent transition metal atoms, resembling the DJ type. The parent material for the present work, $NaLaTiO_4$, can be called the $n = 1$ member ($A' = Na$ and La; B = Ti). Figure 1 shows that the structure of $NaLaTiO_4$ is composed of alternate NaO and LaO layers

(24) (a) Blasse, G. *J. Inorg. Nucl. Chem.* **1968**, *30*, 656. (b) Byeon, S.-H.; Park, K.; Itoh, M. *J. Solid State Chem.* **1996**, *121*, 430. (c) Toda, K.; Kameo, Y.; Kurita, S.; Sato, M. *J. Alloys Compd.* **1996**, *234*, 19.

(25) (a) Byeon, S.-H.; Yoon, J.-J.; Lee, S.-O. *J. Solid State Chem.* **1996**, *127*, 119. (b) Toda, K.; Kurita, S.; Sato, M. *Solid State Ionics* **1995**, *31*, 107.

(26) McIntyre, R. A.; Falster, A. U.; Li, S.; Simmons, W. B.; O'Connor, C. J.; Wiley, J. B. *J. Am. Chem. Soc.* **1998**, *120*, 217.

(27) Izumi, F.; Murata, H.; Watanabe, N. *J. Appl. Crystallogr.* **1987**, *20*, 411.

(28) Gopalakrishnan, J.; Bhat, V. *Inorg. Chem.* **1987**, *26*, 4299.

arranged in the sequence $-(NaO)_2-TiO_2-(LaO)_2-TiO_2-$ along the c axis. A relative displacement of adjacent TiO_6 octahedral layers along the (110) direction leads to a staggered conformation with respect to each other. In contrast to $n > 1$ members, the two different A' layers (Na and La layers) with the rock-salt-type structure in this member results in a strong charge imbalance between layers. Moreover, an ion-exchange reaction in only one layer (Na layer) also induces a significant structural imbalance between the layers because only the exchanged layer has strongly contracted spaces, as well as 50% vacant sites. Exchange reactions accompanied by such an unfavorable change led to the decomposition of the products when the reaction was carried out at higher temperature. These reactions were also sensitive to the physical conditions such as reaction time and temperature fluctuations during reaction. Sufficiently low and constant temperature was therefore required for the exchange reaction. Exchanges in aqueous solutions of several transition metal salts were unsuccessful.

Structure Refinement. The unit cell parameters of $NaLaTiO_4$ prepared as a parent oxide for the ion-exchange reaction were $a = 3.772(1)$ Å and $c = 13.023(2)$ Å (space group $P4/nmm$), which are in good agreement with the values previously reported.²⁴ The X-ray diffraction patterns of $M^{II}_{0.5}LaTiO_4$ ($M = Co, Cu, \text{ and } Zn$) showed strong low-angle reflections, and their similarity to the pattern of the parent oxide suggested that the layer-type structure was retained after the exchange reaction. All of the reflections of $M^{II}_{0.5}LaTiO_4$ were accordingly indexed according to a tetragonal symmetry. A contraction along the c axis with respect to the parent $NaLaTiO_4$ was consistent with the exchange of sodium ion by much smaller transition metal ions. No systematic extinction was observed for the hkl reflections, leading to the P -type unit cell of several possible space groups. A number of possible tetragonal space groups consistent with the primitive cell were tested, and the two space groups ($P4mm$ and $P4/nmm$) giving the best reliability factors were selected.

To determine the most probable space group for $M^{II}_{0.5}LaTiO_4$, structure refinement for $Zn_{0.5}LaTiO_4$ was carried out using its neutron diffraction pattern. Refinement based on the space group $P4mm$ gave satisfactory results, but several linear constraints were required, and relatively large temperature parameters were observed for some oxygen atoms. In contrast, although determination of the systematic absences by the glide plane, and thus the space group, was not clear, a probable extinction rule of $h + k = 2n$ could be detected for $hk0$ reflections. Hence, the crystal structure of $Zn_{0.5}LaTiO_4$ was examined again using the initial atomic positions (space group $P4/nmm$) of the parent $NaLaTiO_4$.²⁴ Because the 1:2 exchange reaction between divalent and monovalent ions must give rise to a cation deficiency in the interlayer spaces of the parent oxide, the occupancy factor of Zn for the position $2c$ was kept at 0.5 during refinement. In this structure, divalent metal ions would thus be statistically distributed at one-half of the sodium positions in $NaLaTiO_4$. Such a site in the NaO rock-salt-type layer might be unsuitable for small transition metal cations because it is coordinated by nine oxygen ions. Indeed, this refinement gave poor

Table 1. Crystallographic Data of $M^{II}_{0.5}LaTiO_4$, where $M = Co, Cu, \text{ and } Zn$

	$Co_{0.5}LaTiO_4^a$	$Cu_{0.5}LaTiO_4^a$	$Zn_{0.5}LaTiO_4^b$
space group	$P4/nmm$	$P4/nmm$	$P4/nmm$
a (Å)	3.71379(6)	3.73606(9)	3.7234(1)
c (Å)	12.7016(2)	12.0736(3)	12.7488(6)
Z	2	2	2
V (cm ³)	175.2	168.5	176.8
ρ (g/cm ³)	5.31	5.57	5.33
R_i (%)	3.26	4.46	3.81
R_{wp} (%)	10.41	8.74	5.55
R_p (%)	8.02	6.77	4.27
R_E (%)	6.23	5.62	3.11

^a X-ray diffraction data. ^b Neutron diffraction data; wavelength of neutron = 1.8346 Å.

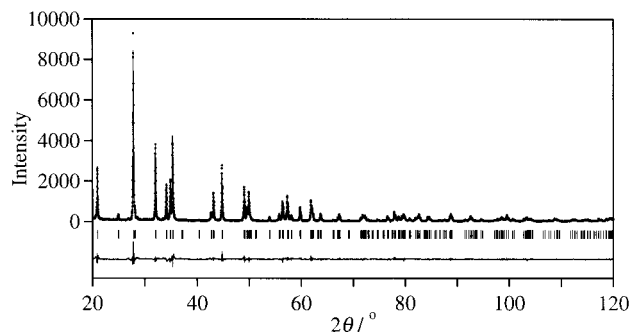


Figure 2. Calculated (solid line), experimental (dotted line), and difference (solid line on the bottom) X-ray powder diffraction patterns of $Co_{0.5}LaTiO_4$.

reliability factors and large or negative isotropic temperature factors.

Using ion-exchange reaction methods, a series of layered oxides $A'[A_{n-1}M_nO_{3n+1}]$, which is closely related to the typical RP phase $A_{n+1}M_nO_{3n+1}$, was generated for $A' = Li, Na, Ag, Co, Cu, Zn$; $A = La, Ca$; and $M = Nb, Ti$.^{4,23,29-31} Two successive perovskite layers in these oxides are brought closer together so that tetrahedral sites are induced, forming half-occupied $A'O$ tetrahedral layers instead of AO rock-salt layers. Such a tetrahedral layer model was adopted for better refinement of $Zn_{0.5}LaTiO_4$. Hence, when the position of Zn was shifted to $2a$ (0.0, 0.0, 0.0) rather than $2c$ (0.0, 0.5, z), the refinement rapidly converged in the space group $P4/nmm$ to excellent profile fit parameters. The occupancy factor of Zn was also kept at 0.5 during refinement because of the cation deficiency in the ZnO_4 tetrahedral layer spaces.

Similarly to the case of the neutron diffraction pattern for $Zn_{0.5}LaTiO_4$, the refinement of X-ray diffraction patterns for $M^{II}_{0.5}LaTiO_4$ ($M = Co \text{ and } Cu$) converged easily and gave agreeable crystallographic parameters when the $P4/nmm$ space group was adopted and Zn was replaced by Co or Cu. Corrections for the $(00l)$ preferred orientation were made for both phases in the final stage of the refinement. Some crystallographic data and the final reliability factors, which were determined by X-ray and neutron diffraction, are given in Table 1. The observed, calculated, and difference profiles for all phases are plotted in Figures 2–4. The refined atomic

(29) Sato, M.; Abo, J.; Jin, T.; Ohta, M. *J. Alloys Compd.* **1993**, *192*, 81.

(30) Sato, M.; Watanabe, J.; Uematsu, K. *J. Solid State Chem.* **1993**, *107*, 460.

(31) Toda, K.; Sato, M. *J. Mater. Chem.* **1996**, *6*, 1067.

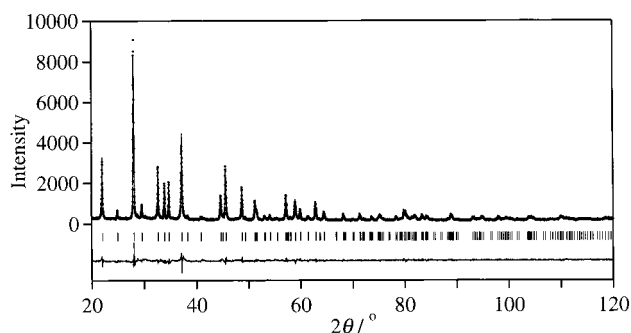


Figure 3. Calculated (solid line), experimental (dotted line), and difference (solid line on the bottom) X-ray powder diffraction patterns of $\text{Cu}_{0.5}\text{LaTiO}_4$.

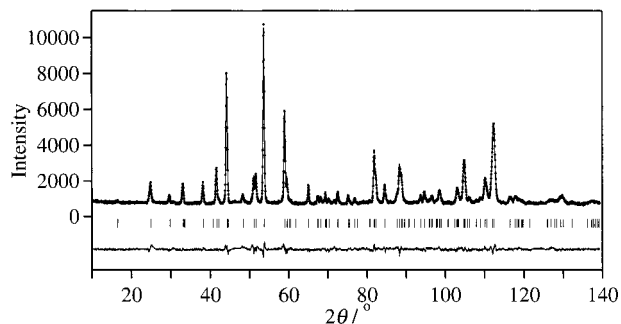


Figure 4. Calculated (solid line), experimental (dotted line), and difference (solid line on the bottom) neutron powder diffraction pattern of $\text{Zn}_{0.5}\text{LaTiO}_4$.

Table 2. Atomic Positions and Isotropic Temperature Factors of $\text{M}_{0.5}\text{LaTiO}_4$ (M = Co, Cu, and Zn)

compound	atom	g^c	x	y	z	B (Å ²)
$\text{Co}_{0.5}\text{LaTiO}_4^a$	Co	0.5	0.0	0.0	0.0	1.01(9)
	La	1.0	0.0	0.5	0.38528(7)	0.27(2)
	Ti	1.0	0.0	0.5	0.7887(2)	0.14(5)
	O(1)	1.0	0.0	0.0	0.2498(4)	0.4(1)
	O(2)	1.0	0.0	0.5	0.5754(7)	0.6(2)
$\text{Cu}_{0.5}\text{LaTiO}_4^a$	O(3)	1.0	0.0	0.5	0.9334(7)	1.8(2)
	Cu	0.5	0.0	0.0	0.0	1.09(9)
	La	1.0	0.0	0.5	0.37910(9)	0.71(4)
	Ti	1.0	0.0	0.5	0.8017(3)	0.65(8)
	O(1)	1.0	0.0	0.0	0.2383(5)	0.9(3)
$\text{Zn}_{0.5}\text{LaTiO}_4^b$	O(2)	1.0	0.0	0.5	0.5868(8)	0.7(3)
	O(3)	1.0	0.0	0.5	0.9537(9)	1.7(3)
	Zn	0.5	0.0	0.0	0.0	1.62(9)
	La	1.0	0.0	0.5	0.3845(2)	0.13(5)
	Ti	1.0	0.0	0.5	0.7877(3)	0.14(9)
	O(1)	1.0	0.0	0.0	0.2513(2)	0.42(5)
	O(2)	1.0	0.0	0.5	0.5757(2)	0.22(6)
	O(3)	1.0	0.0	0.5	0.9301(3)	1.89(8)

^a X-ray diffraction data. ^b Neutron diffraction data; wavelength of neutron = 1.8346 Å. ^c Occupancy factor.

coordinates and isotropic temperature factors are listed in Table 2.

Structural Description. Selected bond lengths and bond angles for $\text{M}_{0.5}\text{LaTiO}_4$ (M = Co, Cu, and Zn) are compared with those of the parent NaLaTiO_4 in Table 3. The ideal structure for $\text{M}_{0.5}\text{LaTiO}_4$, illustrated in Figure 5, is characterized as a two-dimensional framework of LaTiO_4 layers perpendicular to the c axis. Except for the fact that single perovskite layers consisting of corner-sharing TiO_6 octahedra are separated by transition metal layers instead of alkali metal layers, the overall structural characteristics of the parent NaLaTiO_4 (Figure 1) are retained after the exchange reaction. The adjacent perovskite blocks have staggered

Table 3. Comparison of Selected Bond Lengths (Å) and Bond Angles (°) in Parent NaLaTiO_4 and $\text{M}_{0.5}\text{LaTiO}_4$ (M = Co, Cu, and Zn)

	NaLaTiO_4^a	$\text{Co}_{0.5}\text{LaTiO}_4^b$	$\text{Cu}_{0.5}\text{LaTiO}_4^b$	$\text{Zn}_{0.5}\text{LaTiO}_4^c$
bond lengths				
M–O(3) (×4)		2.042(3)	1.950(3)	2.064(2)
Ti–O(1) (×4)	1.953	1.920(2)	1.929(2)	1.927(1)
Ti–O(2) (×1)	2.66	2.678(8)	2.594(9)	2.703(5)
Ti–O(3) (×1)	1.72	1.833(8)	1.835(9)	1.816(6)
La–O(2) (×4)	2.719	2.674(2)	2.674(2)	2.673(2)
La–O(2) (×1)	2.37	2.415(8)	2.508(9)	2.438(4)
La–O(1) (×4)		2.532(4)	2.526(3)	2.521(4)
bond angles				
O(3)–M–O(3)		131.0(4)	146.7(6)	128.9(2)
		99.9(2)	94.7(2)	100.74(7)
O(1)–Ti–O(1)	154.3	150.6(4)	151.1(4)	150.1(3)
		86.3(1)	86.4(1)	86.18(7)

^a Reference 24b. ^b X-ray diffraction data. ^c Neutron diffraction data.

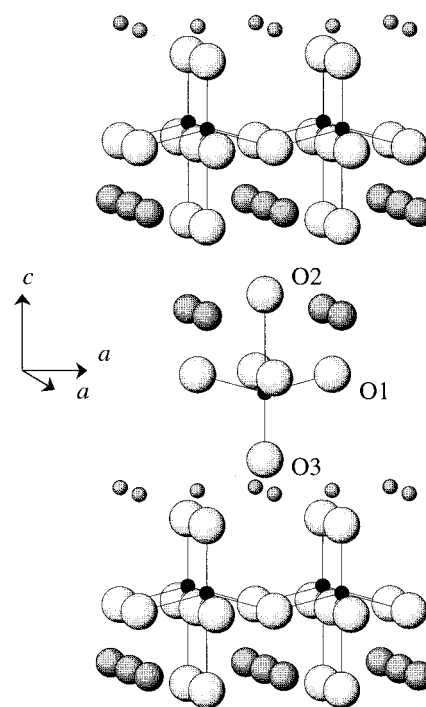


Figure 5. Idealized structure of $\text{M}_{0.5}\text{LaTiO}_4$ (M = Co, Cu, and Zn) represented perpendicular to the c direction of the tetragonal unit cell. Only Ti–O bonds are shown by lines (M = small shaded spheres, La = large shaded spheres, Ti = small black spheres, and O = large white spheres).

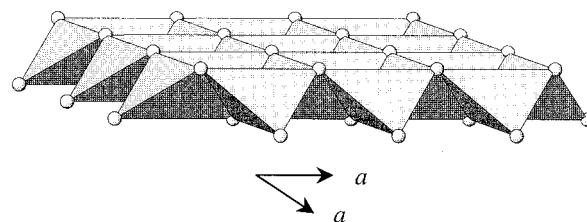


Figure 6. Schematic view of MO_4 tetrahedral linkages in the interlayer spaces of $\text{M}_{0.5}\text{LaTiO}_4$. One-half of tetrahedral sites are statistically occupied by the M atoms. Small spheres represent the oxygen atoms.

conformations with respect to each other, and a displacement of the Ti atom from the center of its octahedron toward the transition metal layers gives a strongly distorted TiO_6 octahedron involving one short Ti–O(3) bond, one long Ti–O(2) bond, and four normal-length

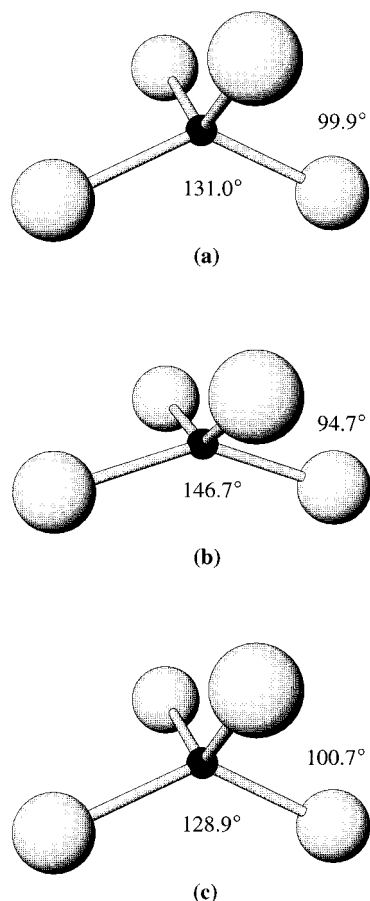


Figure 7. Tetrahedral coordination surrounding M atom in $M_{0.5}LaTiO_4$: (a) CoO_4 , (b) CuO_4 , and (c) ZnO_4 . Small and large spheres represent M and O, respectively.

Ti–O(1) bonds. The empirical expression for the bond valence, $\nu_{ij} = \exp[(R_{ij} - d_{ij})/b]$, where R_{ij} and d_{ij} are the bond valence parameter and bond length, respectively, has been widely adopted to estimate valences in inorganic solids.³² The calculated bond valences for titanium in $M = Co, Cu,$ and Zn compounds are 4.06, 4.01, and 4.04, respectively, in excellent agreement with the theoretical valence of 4. If we consider the valence for $Cu_{0.5}LaTiO_4$ as an example, the individual contributions are $\nu_{Ti-O(1)} = 0.735$, $\nu_{Ti-O(3)} = 0.947$, and $\nu_{Ti-O(2)} = 0.122$. The contribution of $\nu_{Ti-O(2)}$ to the total value of ν_{Ti} is very small, in agreement with the very long Ti–O(2) bond.

Figure 6 shows a schematic arrangement of tetrahedra occupied by transition metal atoms in the interlayer spaces. They are surrounded by four O(3) atoms, forming the edge-sharing MO_4 tetrahedral layer. One-half of these tetrahedral sites are statistically occupied by transition metal atoms. If we compare the lattice constants, contractions of 2.5, 7.3, and 2.1% along the c axis and 1.5, 1.0, and 1.3% in the ab plane were induced by the exchange reaction for $M = Co, Cu,$ and Zn , respectively. The most significant contraction along the c axis for the Cu analogue should arise from the d^9 electronic configuration of Cu^{II} , which is expected to show local structural compression at the tetrahedral site. The Jahn–Teller theorem³³ predicts that the d^4

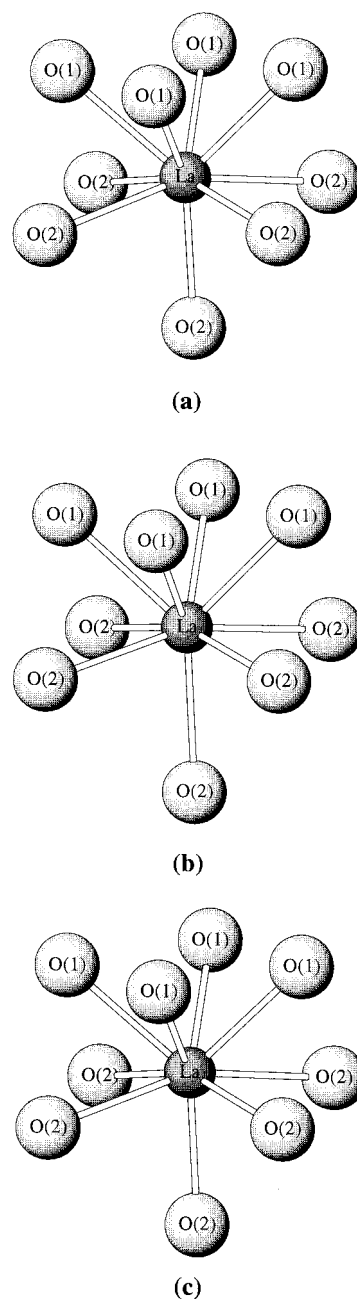


Figure 8. Coordination polyhedra around the La atom in (a) $Co_{0.5}LaTiO_4$, (b) $Cu_{0.5}LaTiO_4$, and (c) $Zn_{0.5}LaTiO_4$.

and d^9 electronic configurations cause a flattening of the tetrahedron because one of the t_2 orbitals has one fewer electron than the other two. The coordination environments around the Co, Cu, and Zn atoms are shown in Figure 7. Two kinds of O–M–O bond angles are significantly different from the 109.5° angle for a perfect tetrahedron; that is, the tetrahedra are strongly flattened along the c axis. In particular, the strongest flattening is observed for the CuO_4 tetrahedron, as expected. On the other hand, the $(LaO)_2$ layer is almost independent of the nature of transition metal layers. As shown in Figure 8, the coordination polyhedra around La atoms are quite regular, and no considerable difference is observed along with three compounds. The calculated valences for lanthanum are 3.06, 2.97, and 3.07 for $M = Co, Cu,$ and Zn , respectively, which are also very close to the expected value.

(32) Brese, N. E.; O'Keeffe, M. *Acta Crystallogr. B* **1991**, *47*, 192.

(33) Jahn, H. A.; Teller, E. *Proc. R. Soc. London A* **1937**, *161*, 220.

Conclusion

The syntheses of $M^{II}_{0.5}LaTiO_4$ and $M^{II}La_2Ti_3O_{10}$ (M = transition metals) have demonstrated that the alkali metal ions in the interlayer spaces of layered perovskite can be exchanged by divalent transition metal ions under controlled reaction conditions regardless of the thickness (the number of corner-sharing TiO_6 octahedra along the *c* axis) of the perovskite layer. This represents the existence of the new family $M^{II}[A_{n-1}B_nO_{3n+1}]$, which corresponds to a modified RP and DJ series. In contrast to the other members of typical RP and DJ series, the $M^{II}[A_{n-1}B_nO_{3n+1}]$ family, where M is a transition metal, shows various colors depending on the nature of the M layers. Thus, a study of the photocatalytic activity of this family in the visible

range would be challenging. Recently, many series of layered oxides have been reported. Some members of these series could be referred to as $Li_2[A_xB_nO_{3n+1}]^{19}$ and $Li_2[Sr_{n-1}M_nO_{3n+1}]^{20}$ including the reduced niobate $Rb_2LaNb_2O_7^{10}$ and the reduced tantalates $Li_2LaTa_2O_7$, $Li_2Ca_2Ta_3O_{10}$, and $Na_2Ca_2Ta_3O_{10}$.¹⁸ Our results imply that diverse families of different colors and physical properties can be developed by a topotactic exchange reaction between alkali metal ions and transition metal ions in the galleries of these members.

Acknowledgment. This work was supported by Grant R01-2001-00045 from the Korea Science & Engineering Foundation.

CM010962K